ACS OMEGA

http://pubs.acs.org/journal/acsodf

Article

Effect of Degumming Duration on the Behavior of Waste Filature Silk-Reinforced Wheat Gluten Composite for Sustainable Applications

Papiya Bhowmik, Ravi Kant,* and Harpreet Singh

Cite This: *ACS Omega* 2023, 8, 6268−6278

Read Online

ACCESS | Metrics & More | Article Recommendations

ABSTRACT: Silkworm silk proteins are of great importance in several fields of science owing to their outstanding properties. India generates waste silk fibers, also known as waste filature silk, in abundance. Utilizing waste filature silk as reinforcement in biopolymers enhances its physiochemical properties. However, the hydrophilic sericin layer on the surface of the fibers makes it very difficult to have proper fiber−matrix adhesion. Thus, degumming the fiber surface allows better control of the fiber properties. The present study uses filature silk (*Bombyx mori*) as fiber reinforcement to prepare wheat gluten-based natural composites for low-strength green applications. The fibers were degummed in sodium hydroxide (NaOH) solution from a 0 to 12 h duration, and composites were prepared from them. The analysis exhibited optimized fiber treatment duration and its effect on the composite properties. The traces of the sericin layer were found before 6 h of fiber treatment, which interrupted homogeneous fiber−matrix adhesion in the composite. The X-ray diffraction study showed enhanced crystallinity of the degummed fibers. The FTIR study of the prepared composites with degummed fibers showed that shifted peaks toward lower wavenumbers supported better bonding among the constituents. Similarly, the tensile and impact strength of the composite made of 6 h of degummed fibers showed better mechanical properties than others. The same can be validated with the SEM analysis and TGA as well. This study also showed that prolonged exposure to alkali solution reduces the fiber properties, thus reducing composite properties too. As a green alternative, the prepared composite sheets can potentially be applied in manufacturing seedling trays and one-time nursery pots.

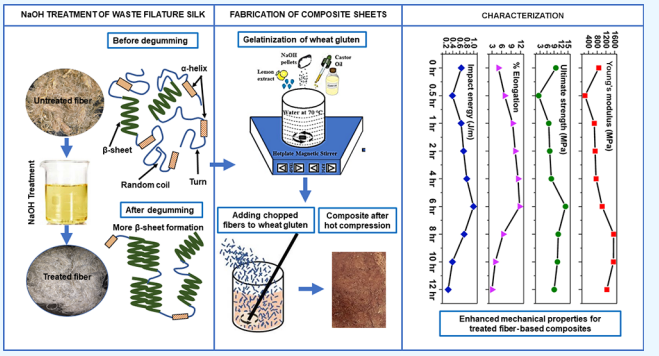

1. INTRODUCTION

Wheat gluten is a natural polymer consisting of a complex protein structure. Because of its high biodegradability, low cost, non-toxicity, and renewability, it is often considered a potential substitute for synthetic resins in natural composites.[1,2] Regardless of its impeccable properties, wheat gluten is very brittle in nature and absorbs ample amounts of moisture after processing. However, these shortcomings can be tailored by introducing synthetic or natural fibers as fiber reinforcements into it.[3−5] Natural fibers are fundamentally sustainable considering their fast biodegradability, non-toxicity, fast renewability, minimum carbon emission, and significantly fewer health hazards.[6] Natural silk (*Bombyx mori*) is one of the most popular fiber reinforcements to produce natural protein-based green composites.[7,8] The waste natural silk, also known as waste filature silk (WFS), produced in textile industries during silk processing, possesses excellent mechanical and thermal properties.[9−12] India is the second-highest silk manufacturer after China on the global map.[13] Along with the production of high-end clothing, the Indian silk industry generates huge silk waste yearly, making it an economical option to use as fiber reinforcement.[14,15] The well-aligned internal structure of the filature silks makes them susceptible to more tensile load, high elongation, and good resilience.[16] Due to long chains of amino acids, these silks possess higher heat resistance capacity.[17] The WFS consists of two parts, fibroins (75%) in the inner section and sericin (25%) on the outer layer. The silk fibroins have a semicrystalline structure that provides inner strength to the silk fibers, and sericin acts like amorphous glue, holding the fibroins and structure together.[18] Among the 18 amino acids that sericin possesses, serine aspartic acid and glycine are the three most essential amino acids responsible for its extreme hydrophilicity.[19,20] Research showed that hydrophobic surfaces

Received: September 14, 2022
Accepted: December 30, 2022
Published: February 10, 2023

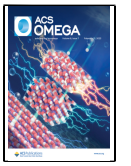

https://doi.org/10.1021/acsomega.2c05963
ACS Omega 2023, 8, 6268−6278

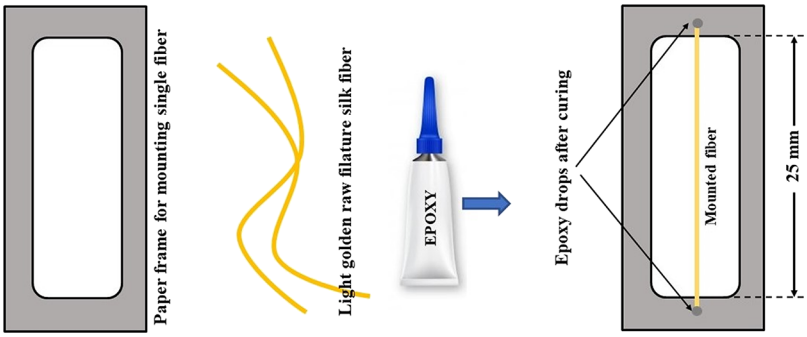

Figure 1. Schematic of sample preparation for the single-fiber tensile test.

bond with proteins more definitely than hydrophilic surfaces. Hydrophobic surfaces attach to another hydrophobic surface more viciously because of a good adsorption process.[21] Because of the hydrophilicity of the sericin layer, it is often challenging to have proper fiber−matrix adhesion with natural polymers like wheat gluten.[19] Although removing the sericin layer reduces the toughness of the silk fiber, the process may benefit the fiber−matrix bonding, thus improving the overall composite properties. The sericin layers can be removed by various degumming methods like washing the fibers off with different solutions like sodium hydroxide (NaOH)[22] and sodium carbonate,[23] soap washing,[24] succinic acid, urea,[25] citric acid,[26] hot water,[27] and hydrogen peroxide.[28] The degummed structure of WFS consists of a random coil amorphous structure and a periodic β-sheet structure. However, the amorphous coil structure may change into a regular β-sheet structure upon mechanical stretching and moisture absorption during the degumming process.[29] Conversion of random and α-helix structures to more β-sheet structures makes the fibers straight, lustrous, and stiffer.[30] The main strength of any natural fiber is acquired from the hydrogen bond present in the core protein structure.[31] Thus, preserving those hydrogen bonds while degumming should be of utmost priority. The degumming process can readily remove sericin layers, but sometimes, too much exposure to the alkali solution may cause detrimental changes to the fiber's mechanical, morphological, and chemical properties. Alkali water solution has been used from ancient times for simple and effective degumming of raw silk cocoons. Alkali degumming removes the sericin binding agent without damaging the nature of the fiber.[32] NaOH and water solution are widely used for deep cleaning, degumming, and enhancing the properties of the raw silk fibers.[22−34] The primary purpose of degumming the raw fiber is to hydrolyze the sericin layer and dissolve it into the degumming solution or media, making it detangled and open.[16,25] When used in developing composites, these detangled fibers help in distributing the stress evenly in the structure, thus improving the overall properties of the composite. Although NaOH treatment improves many properties of the fiber, exposure to the alkali solution for a longer duration disturbs the WFS core structure. Only a handful of studies reported the effect of degumming duration on the texture and core structure of different kinds of silk fibers.[25,32,35,36] The main objective of this study is to optimize the fiber treatment time or degumming time without affecting the core structure of the WFS fibers so that the prepared composites can adhere best to physiochemical properties. In this study, degummed silk fibers were used to prepare a wheat gluten-based biocomposite where the lemon extract was used as a crosslinker and castor oil was used as a plasticizer. The methodology and process optimization to prepare these composite sheets were thoroughly studied in our previous work where the samples were prepared with raw WFS (non-degummed).[11,37] The fibers were treated in 5% NaOH−water solution for 0, 0.5, 1, 2, 4, 6, 8, 10, and 12 h, and the mechanical thermal, morphological, and molecular analysis were done on them.[38,39] For consistency, the NaOH solutions were kept at 5% for all the degumming periods. However, variation of the NaOH concentration for degumming of the fibers is currently out of this paper's scope and is considered a future study. The composite prepared by degummed fibers showed improved physiochemical and thermal properties. It was also observed that extended exposure to alkali solution reduces the fiber and composite properties drastically.

2. METHODOLOGY

2.1. Materials. The WFS was procured from a local vendor in Karnataka, India, at INR 85/kg. The wheat gluten (WG) was procured from Urban Platter, Mumbai, India, whose constituents are 75% protein, 14% carbohydrate, 2% fat, 1% sodium, 1% ash, 6.5% moisture, and 1% ash, the rest of which are impurities as per the manufacturers' catalogue. The pellets of NaOH were procured from Thermo Fisher Scientific Ltd., Mumbai, India, with a 97% purity as per the manufacturer's catalogue. Organic fresh lemon was procured from the local market of Ropar, India, at a nominal rate. 100% natural cold-pressed castor oil was procured from Rey Naturals, Ahmedabad, India.

2.2. Fiber Treatment. An alkali solution was prepared using 5% NaOH and distilled water for degumming the fibers.[22,39,40] The fibers were soaked in the solution for 0.5, 1, 2, 4, 6, 8, 10, and 12 h. The fibers were withdrawn from the solution and washed in distilled water until clean and free from any NaOH residues. The treated fibers (TFs) were semi-dried in natural sunlight and then kept in a hot air furnace at a temperature of 65 °C for 72 h for complete drying. The weight ratio of wet fibers and dry fibers varied between 1.5:1 and 1.3:1 as the gradual removal of sericin.

2.3. Composite Preparation. The fibers were chopped to a length of 20 (±3) mm for preparing the composite. Few fibers from each category were kept intact for the single-fiber tensile test. The single-fiber test specimens were prepared using the paper and glue method, as shown in Figure 1, according to ASTM 3822 standards. The gauge length was kept at 25 mm for all samples as per the ASTM standard, and five samples were tested under each category. The abbreviation used to represent different types of treated and untreated WFS are mentioned in Table 1.

For fabrication of the composite, the WG was mixed with water in a 1:10 ratio. The water was preheated to 70 °C and kept on a hotplate magnetic stirrer to keep the temperature constant while mixing all the constituents. As a dispersion agent of WG,

https://doi.org/10.1021/acsomega.2c05963
ACS Omega 2023, 8, 6268−6278

Table 1. Abbreviation Used to Represent Different Types of Treated and Untreated WFS

name	abbreviation	treatment time (h)
untreated fibers	UF-0	0
30 min of treated fibers	CF-0.5	0.5
1 h of treated fibers	CF-1	1
2 h of treated fibers	CF-2	2
3 h of treated fibers	CF-4	4
4 h of treated fibers	CF-6	6
5 h of treated fibers	CF-8	8
6 h of treated fibers	CF-10	10
7 h of treated fibers	CF-12	12

NaOH pellets were mixed with water at a weight ratio of 2.5% of WG dry matter. Similarly, 2.5% (WG dry matter) of lemon extract was added as a crosslinker to the hot water. For plasticizing the WG, 10% (of WG dry matter) of castor oil was added to the water as well and stirred for 10 min at 200 RPM. The WG was added slowly and gradually to the solution at 500 RPM to avoid cluster formation. After 30 min of continuous stirring, it formed a gluey paste of yellowish texture. The chopped fibers were added to the WG paste and mixed slowly with a stirrer until homogenous dispersion did not occur. The prepared mixture was then spread using the hand-layup process on a nonsticky surface and kept inside a hot air oven at 70 °C until dry. The dried sample sheets had an average thickness of 0.9 (±0.25) mm. The prepared composite sheets were further compressed using hot compression molding at 120 °C and 120 bar for 10 min, followed by 10 min of cold compression. The final fabricated composite sheets were used for various characterization processes. All the composites were prepared using a similar method apart from the fiber types as per the treatment time. The graphical representation of the composite fabrication is shown in Figure 2a,b, where (a) represents the basic methodology to develop the composite sheet and (b) represents the final hot compression process to prepare the composite sheet of fixed thickness. The composition of the prepared samples and the abbreviations used to refer them are mentioned in Table 2.

2.4. Characterization of the Composite. The degummed silk fiber's crystalline structure was examined using an X-ray diffractometer (Anton-Par PANalytical system) with a Cu Kα radiation source in the range of 10−60° (2θ). The tensile strengths of the single fibers were assessed using the Instron 4301(3343) universal tensile tester at room temperature (32 °C) and humidity (67.2%). Additionally, the strain rate was 1 mm/min, and a load cell of 1 kN was used. The mechanical characterization in terms of tensile strength of the prepared WG-WFS composite sheets and mechanical characterization was

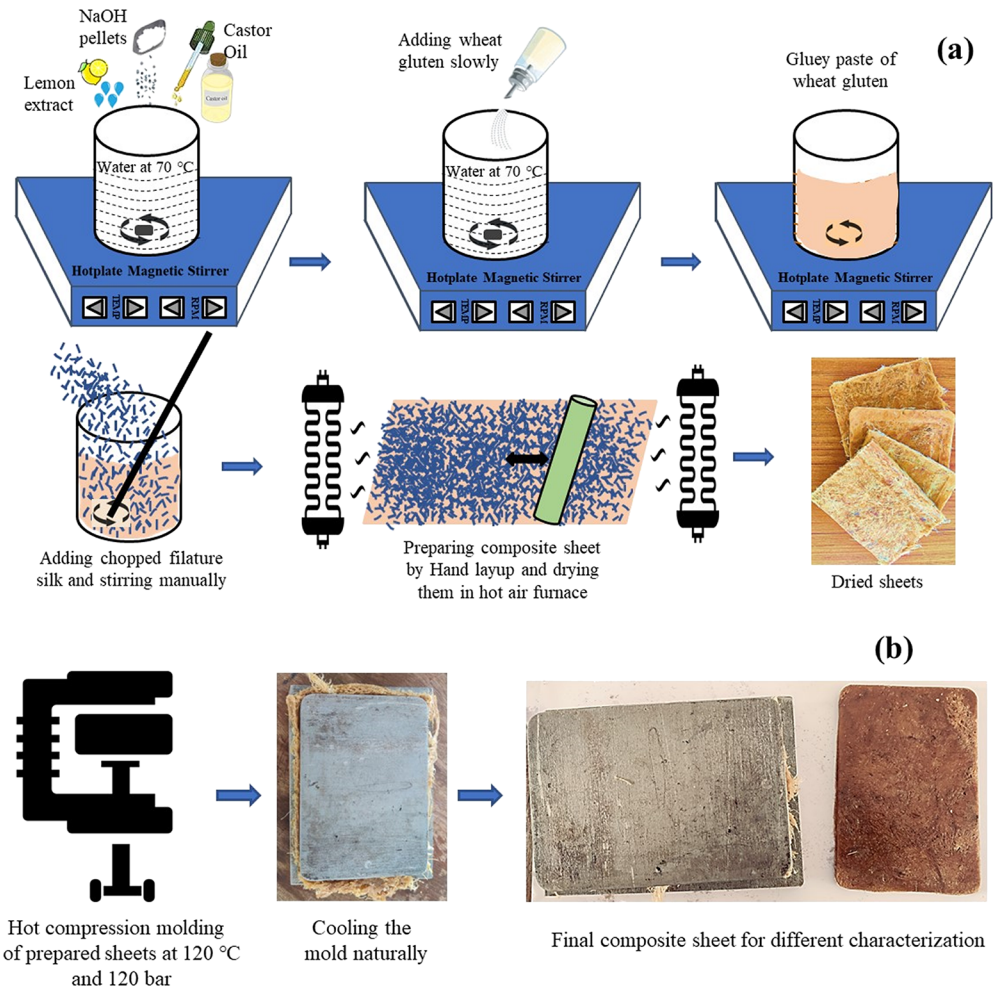

Figure 2. (a) Stages to prepare the primary composite sheets of wheat gluten and treated filature silks. (b) Final composite sheet after hot compression molding.

https://doi.org/10.1021/acsomega.2c05963
ACS Omega 2023, 8, 6268−6278

Table 2. Sample Composition and Abbreviation Used to Represent Different Types of Wheat Gluten and Filature Silk-Based Composites

name	abbreviation	constituents
composite made with the untreated fibers	CUF-0	wheat gluten:filature silk = 50:5010% castor oil, 2.5% NaOH, and 2.5% lemon extract of wheat gluten dry matter
composite made with the 30 min of treated fibers	CTF-0.5	
composite made with the 1 h of treated fibers	CTF-1	
composite made with the 2 h treated fibers	CTF-2	
composite made with the 4 h of treated fibers	CTF-4	
composite made with the 6 h of treated fibers	CTF-6	
composite made with the 8 h of treated fibers	CTF-8	
composite made with the 10 h of treated fibers	CTF-10	
composite made with the 12 h of treated fibers	CTF-12	

conducted using UTM Tinius Olsen H50KS of capacity 50 kN. The strain rate was kept at 2 mm/min, where the load cell was 5 kN. The samples were prepared following ASTM D412 standards, where each test was repeated four times, and average values were reported. The average values of Young's modulus, tensile strength, and percentage elongation for different samples were compared and reported. The impact strength of the composite was analyzed using the Izod impact test using the Rockwell hardness testing machine according to ASTM D785-98 standards. The sample size was 63.5 mm × 12.7 mm × 3 mm with a v-notch at the middle. The impact energy was calculated in the Izod scale (J/m). The SEM micrographs were studied using a JSM-7500F field emission scanning electron microscope. As the samples were nonconductive, they were platinum-coated by JEOL JFC-1600 Auto for 20 s prior to FFSEM analysis. The thermal properties of the prepared composites were tested by a Mettler Toledo thermogravimetric analyzer (TGA) in the range of room temperature to 620 °C. The initial weight of the samples was 5 mg, and the heating rate was 10 °C/min. The functional groups and degree of interaction between the composite constituents were studied using Fourier transform infrared spectroscopy using Bruker Tensor II in the range of 400−4000 cm^{-1}. As WG is more susceptible to moisture, all the samples were cleaned with ethanol and kept in a vacuum furnace at 60 °C for 24 h prior to every characterization.

3. RESULTS AND DISCUSSION

3.1. XRD Analysis of the Fibers. XRD analysis was performed on all the silk samples before and after degumming to study the change in crystalline and amorphous structure in the WFS for different conditions. It is shown in Figure 3 that the major diffraction peaks got generated at 21° (2θ), which generally depicts the secondary β-structure or crystallinity of the fibers. It is observed that the raw silk fiber UF-0 showed a broad peak around 21.3°, which indicated the natural pattern of amorphous silk. As degumming begins, the peak intensity increases gradually from CF-0.5 to CF-10. The increase in peak intensity and height conveys the increase in the crystallinity of the fibers upon degumming.[41] However, the peak intensity drops slightly for CF-12, imparting that over-exposure to NaOH solution may have started to affect the core structure of the silks. Table 3 quantifies the percentage of amorphous and crystalline structure for all the fibers as per the XRD-generated data.

3.2. Fourier Transform Infrared (FTIR) Spectroscopy. Building strong interfacial cohesion between silk fibroins and the adjacent polymer is challenging. Removing the sericin layer of silk by NaOH treatment improves the composite's overall properties. FTIR shows the underlying factors of structural

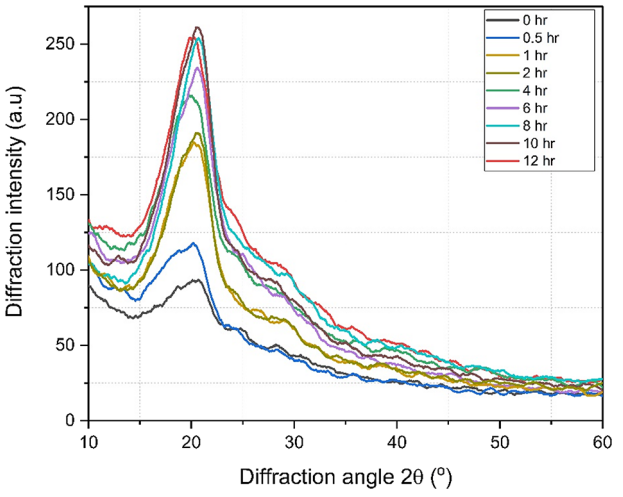

Figure 3. X-ray diffraction curves of the waste filature silk before and after degumming in NaOH solution for different duration of time.

Table 3. Change in Percentage of Crystallinity and Amorphous Region of Waste Filature Silk before and after Degumming in NaOH Solution for Different Durations

sample name	% crystallinity	% amorphous
UF-0	38.5	61.5
CF-0.5	39.4	60.6
CF-1	40.4	59.6
CF-2	40.9	59.1
CF-4	43.7	56.3
CF-6	44.8	55.2
CF-8	48.4	51.6
CF-10	48.9	51.1
CF-12	47.0	53

changes to understand the variation in mechanical properties of the prepared composites. Hence, FTIR spectra are used here to identify the structure of untreated fiber (UF), simple WG, treated fiber (TF), and the composites prepared by them. The primary structure of the silk consists of amino acids of glycine, alanine, and serine in a repetitive order.[16] They take up to 90% of the protein in silk, and the last 10% consists of glutamic, valine, and aspartic acids.[35] They act like side chains and are primarily responsible for the elasticity and strength of the silk. The secondary structure of the silk is mainly dominated by β-pleated sheets connected to each other with hydrogen bonds.[42] Apart from this, α-helix, turn, and random coils also play a dominating part in the secondary structure of silk. FTIR spectra are widely

https://doi.org/10.1021/acsomega.2c05963
ACS Omega 2023, 8, 6268−6278

sensitive to the secondary structure of silk fibroins, providing molecular validation of the change in silk structure.[43,44] The signature absorption peaks for WFS are found around 1620 cm^{-1} (Amide I), 1515 cm^{-1} (Amide II), and 1260 cm^{-1} (Amide III). These peaks are conformation peaks of the crystalline β sheet structure, and the silk shows similar peaks in all degumming conditions until the core structure starts to break.[36] The Amide I band of the silk fibroin (between 1600 and 1700 cm^{-1}) is mainly associated with C=O stretching vibration (70 to 85%) and is directly related to the backbone conformation. The Amide II band results from the N−H bending vibration (40−60%) and the C−N stretching vibration (18−40%). The Amide III band is conformationally sensitive and very rarely traced with sharp peaks. The Amide II peaks are found where microsphere or aqueous formation takes place. The formation of microspheres confirms a more stable state of the fibroins. The stretched vibration peaks around 1600 cm^{-1} confirm the presence of stronger C=O stretching. The definite peaks for the Amide I and Amide II regions at 1630 and 1520 cm^{-1} indicate crystalline β-sheet conformation.[45] As the degumming occurs, some subtle change occurs around 1000 cm^{-1}, as shown in Figure 4. The peak intensity increases for the

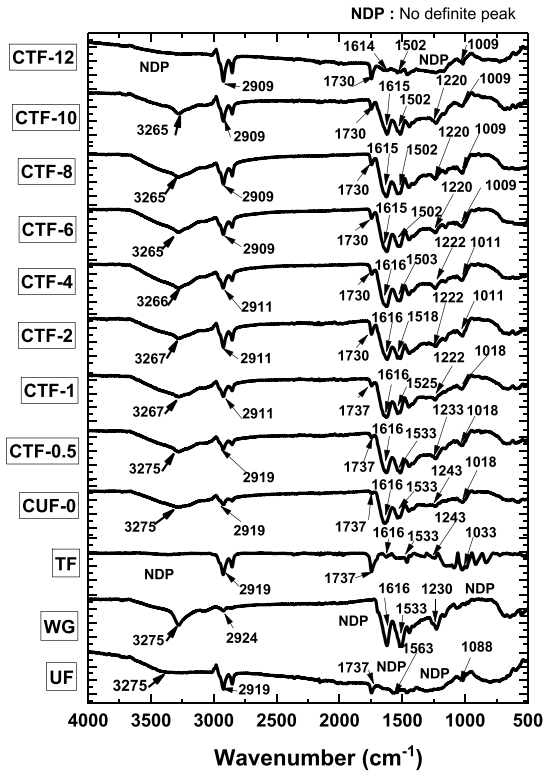

Figure 4. Comparison graph of FTIR analysis between treated and untreated waste filature silk, wheat gluten, and the composites prepared by them.

TFs, indicating enhanced crystalline β structure formation.[36] Degumming generally increases the formation of crystalline β-sheets of WFS. Although lesser exposure to NaOH treatment does not affect the amorphous peptide formation of the silk, prolonged exposure of silk to alkali solution may affect the silk surface morphology.[32,46] The alkali treatment removes the amorphous region and makes the silk more crystalline, thus reducing the silk elongation rate. Increasing the duration of fiber treatment reduces the elongation and creates more brittleness in the WFS and the composites. The gelatinization of WG occurs in the presence of lemon extract, NaOH, and castor oil. These components help to have better crosslinking in the WG and WG with WFS. Better crosslinking leads to better interaction between functional and proton donor groups. Enhanced interaction forces the proton donor group to make them give up their electron and reduce electron density. Reduced electron density also reduces the vibrational energy of the different functional groups, thus generating characteristic peaks at lower wavenumbers.[47] The signature peaks of lower wavenumber in FTIR studies indicate better interaction among the constituents of the matrix.[11] The reduced intensity of WG to CUF-0 at 3200 peaks represents reduced hydroxyl groups after crosslinking. The peaks between 1613 and 1632 cm^{-1} are assigned for β-sheets of the WG protein structure. The β structure changes with the increase in hydration. The spectra generated around 1000 cm^{-1} are the combined peaks for WG and WSF both. The peaks and their absorption range are represented in Table 4. The

Table 4. FTIR Absorption Band of Different Compound Classes Present in Filature Silk and Wheat Gluten Composites[48]

absorption (cm^{-1})	appearance	group	compound class
3300−2500	strong broad	O−H stretching	carboxylic acid
3000−2800	strong broad	N−H stretching	amine
1750−1725	strong	C=O stretching	esters
1650−1580	medium	N−H bending	amine
1550−1500	strong	N−O stretching	nitro compound
1250−1020	medium	C−N stretching	amine
1085−1050	strong	C−O stretching	primary alcohol

tensile and thermal properties of the composites increase because of the presence of opened-up fibroins due to their ability to interact with WG protein to form complex protein structures. The reduced wavenumbers on and after CTF-4 indicated enhanced interaction among the constituents of the composite after the complete removal of the sericin layer. This data also supports the composites' enhanced tensile and thermal properties, as described in the upcoming sections.

3.3. Scanning Electron Micrographs (SEMs). The SEMs showed the microlevel changes in the fibers and composites for all nine sets of samples. The micrographs shown in Figure 5 elaborate on the gradual removal of the sericin layer from the fibers, composite cross section, and adhesion between the major constituents of the composites. Samples were collected from the fractured surface of the composites to study the behavior of fiber−matrix bonding under applied load. Figure 5a shows CUF-0, which clearly shows the thick sericin layer and the heavily tangled fibroins in it. Fiber clustering renders poor mechanical properties. As the untreated WFS shows a hydrophilic nature, the fiber−matrix adhesion was very poor for the prepared composite. The micrograph of the WFS collected from the fractured surface showed lack of adhesion of WG, in the fiber periphery. This slip of fiber from WG results in average mechanical properties. The TFs for the first three samples, CTF-0.5, CTF-1, and CTF-2, had medium to low traces of sericin present in them. The semi-open fibers and the presence of sericin created uneven adhesins of fiber−matrix and interlayer voids, as shown in Figure 5b−d. The samples prepared by TFs from 4 h onward had low to no traces of the sericin layer. The complete removal of sericin made the fibers straighter and more lustrous. This helped to develop a better composite structure

https://doi.org/10.1021/acsomega.2c05963
ACS Omega 2023, 8, 6268−6278

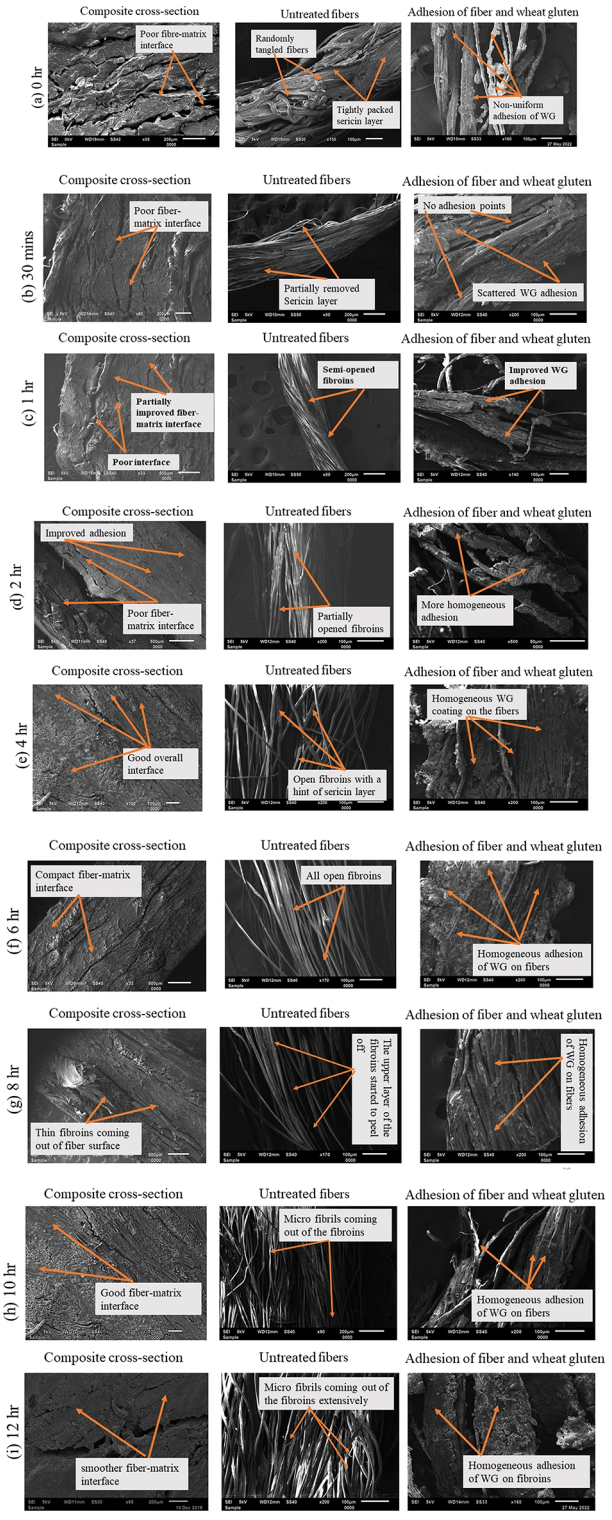

Figure 5. SEM micrograph of (a) CUT-0, (b) CTF-0.5, (c) CTF-1, (d) CTF-2, (e) CTF-4, (f) CTF-6, (g) CTF-8, (h) CTF-10, and (i) CTF-12, analyzing the microstructure of the composite cross section, fibers at different stages, and fiber−matrix adhesion of waste filature silk and wheat gluten.

that was almost free from voids and poor adhesion, as shown in Figure 5e,f. CTF-4 and CTF-6 showed the most promising properties among all their counterparts. The interface is strongest for CTF-6 as it showed the least number of voids and a better interface among all the samples. A better fiber−matrix interface leads to better stress distribution, enhancing the prepared composites' load bearing capacity under tensile and impact loading. Although the fiber−matrix adhesion in CTF-8, CTF-10, and CTF-12 was also good, the fibroins' thinning due to extensive alkali exposure weakened the fibers. As a result, they cannot carry the tensile and impact loads ensuing in easy failure, as seen in Sections 3.4 and 3.5.

3.4. Tensile Properties. The tensile properties of the fibers and composites were compared among the nine sets of samples. The first sample, CUF-0, was prepared from UFs where the sericin layer glued the fibroins randomly. The fibroins were badly tangled and unable to stretch themselves upon tensile loading, resulting in the brittle behavior of the composite.[22] The tensile strength is comparatively higher for CUF-0, but the elongation is critically low, supporting the brittle nature of the composite. The first four sets of TF-based composites CTF-0.5, CTF-1, CTF-2, and CTF-4 showed a gradual increase in their tensile properties, as shown in Figure 7. The micrograph in Section 3.3 clearly showed the partially present hydrophilic sericin layer among the semi-opened fibroins, which delivers uneven sipping of WG into fibers. This leads to the formation of internal voids in the composite, resulting in early failure upon tensile loading. As the sericin layer was completely removed after 6 h of NaOH treatment, the fiber−matrix adhesion improved drastically, resulting in improved tensile properties. The fibers of 6 h of treatment showed improved elastic properties as they were entirely free from gluey sericin binding. It increased the tenacity of the fibers, which increased the interfacial adhesion of the fiber and matrix. Hence, CTF-6 showed the best elongation among all the composites. CTF-8, CTF-10, and CTF-12 showed excellent Young's modulus but drastically reduced maximum tensile strength and elongation. Exposure of the fibers in NaOH solution for a prolonged period resulted in the formation of more β-sheets, making them stiffer.[35] It also started to peel the microfibrils, making the fibers thinner and weaker. It reduced the fibers' strength, which resulted in the samples' early failure. The same characteristic pattern can be seen in the tensile properties of the fibers, as shown in Figure 6. Although the degumming process increased the crystallinity of the fibers, thus making them stiffer, gradual removal of the sericin layer increased the fibers' elongation as they can move freely. It further verified the tensile behavior of the composite influenced by the tensile properties of the fiber as the degumming time increased.

Because of all these reasons, the Young's modulus for CUF-8 is maximum showing enhanced adhesion among the fiber and wheat gluten, but it lacks elongation. As fiber failure occurred drastically upon increased load, wheat gluten overpowered the composite's mechanical properties, thus making it more brittle. The same trend can be seen for CTF-10 and CTF-12. The tensile comparison proved optimized properties for CTF-6 as it showed good Young's modulus, best tensile strength, and elongation among its peers.

3.5. Impact Strength. During the impact test, impact energy gets dissipated in the form of matrix breakage, fiber breakage, matrix−fiber interface failure, delamination of layers, and crushing of the core structure of the composite elements. The impact test finds the damage tolerance of the composite as impact load reduces the design strength of the composite. The low-velocity Izod test primarily finds the damage resistance in terms of absorbed energy or impact energy, which is directly proportional to impact strength. Figure 8 shows that the impact energy for CUF-0 is 0.644, indicating higher impact strength than CTF-0.5 and CTF-1 composites. The sericin layer of the

https://doi.org/10.1021/acsomega.2c05963
ACS Omega 2023, 8, 6268−6278

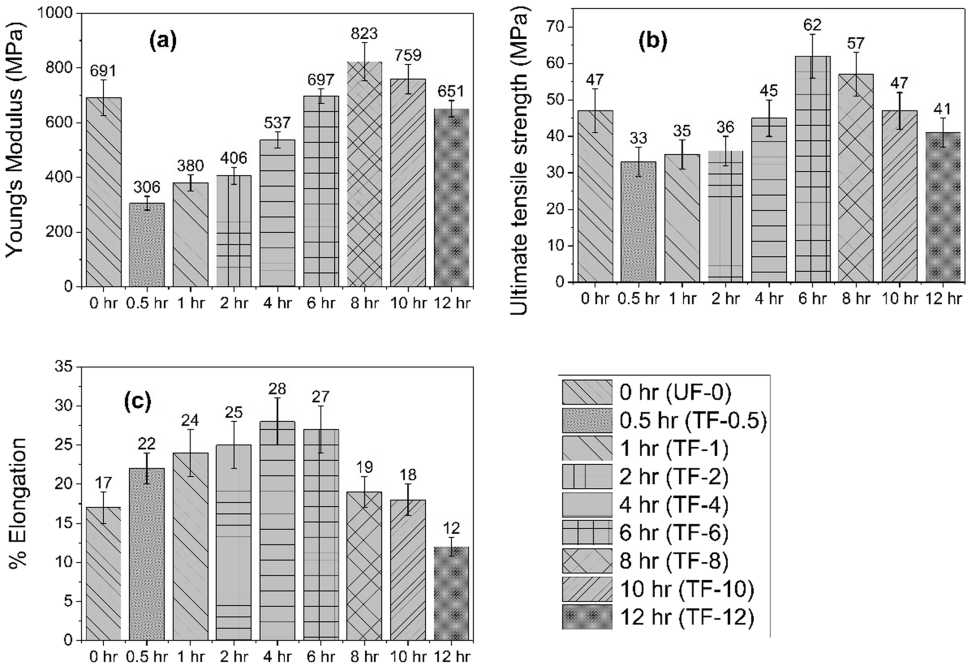

Figure 6. Comparison graph of the single-fiber tensile properties of the waste filature silk before and after treatment. (a) Young's modulus, (b) ultimate tensile strength, and (c) % elongation.

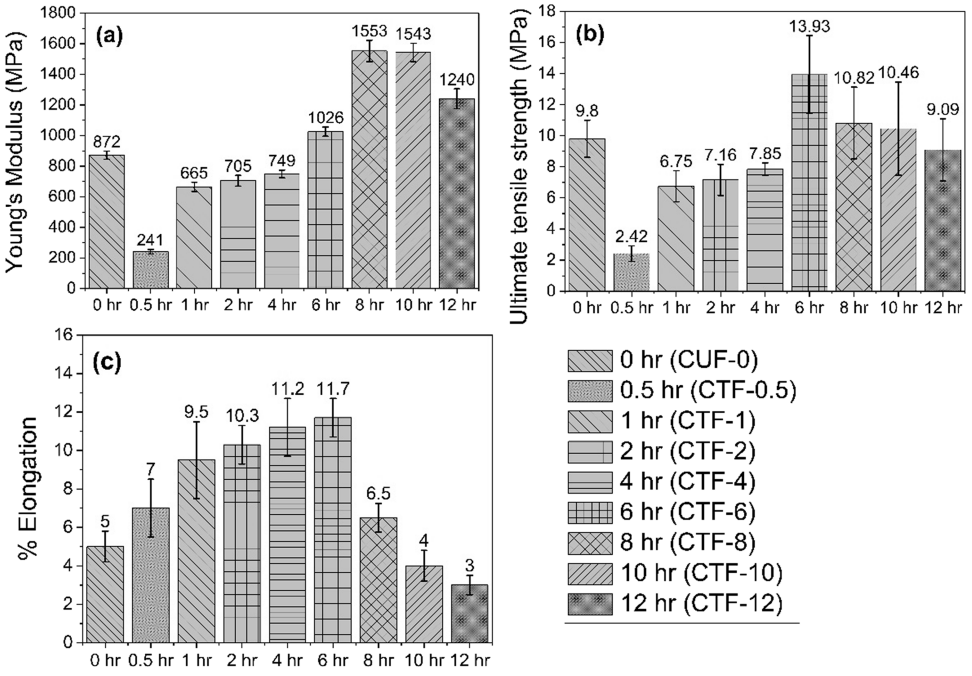

Figure 7. Comparison graph of tensile properties for the composite manufactured by wheat gluten and untreated and NaOH treated waste filature silk. (a) Young's modulus, (b) ultimate tensile strength, and (c) % elongation.

UFs works like external support, increasing the composite's strength. However, at the same time, sericin does not offer good fiber−matrix adhesion with WG, being hydrophilic. The tangled fibers tightly packed under the sericin layer also fail to distribute stress under impact load. This results in the early failure of the composites. On the other hand, CTF-0.5 and CTF-1 show early failure due to randomly removed sericin layers. The semi-opened and semi-tangled fibers fail under impact load due to uneven stress distribution and non-homogeneous orientation of the fibroin. The impact strength increases CTF-2 onward as sericin starts to peel off entirely from the fibers and the fibroins start to untangle. NaOH-TF removes the sericin layer, which activates alanine and glycine compounds. As both these compounds are hydrophobic in nature, it induces a higher affinity toward hydrophobic WG and develops a stronger bond.[22,35] It increases the fiber−matrix interface, thus increasing impact strength. The interface is most substantial for CTF-6 as it showed the best fiber and matrix adhesion and very few voids, as shown in Section 3.3. The impact strength further reduces for

https://doi.org/10.1021/acsomega.2c05963
ACS Omega 2023, 8, 6268−6278

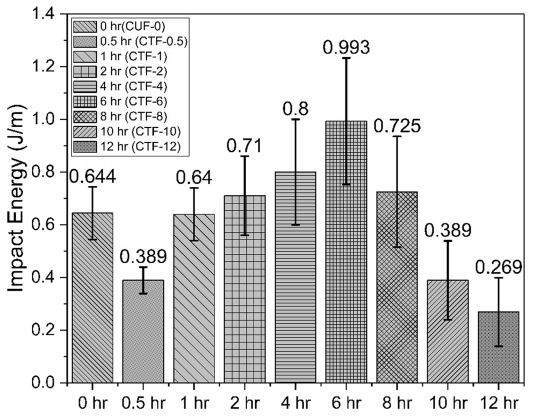

Figure 8. Comparison graph of impact energy for the composite manufactured by wheat gluten and untreated and NaOH treated waste filature silk.

CTF-8, CTF-10, and CTF-12 as the fiber diameter reduces, making them weak and breaking faster under impact.

3.6. TGA. TGA shows the thermal stability of the composites at elevated temperatures. The first stage of 0 to 5% weight reduction occurs due to the evaporation of trapped moisture and air in the voids of the sample. The integral moisture absorption property of WG attracts a lot of residual moisture. This moisture and air evaporate upon heating, which occurs in the first stage of weight reduction. The subsequent 5 to 10% weight reduction occurs due to the evaporation of plasticizer in the composites, which is castor oil for this case. The next stage of drastic weight reduction occurs at the temperature range of 200 to 250 °C, as shown in Figure 9, due to the breakage of amino acid and hydroxyl groups present in the composite. As most of the graphs are overlapping, an enlarged view of the TGA graph at 220 °C is as shown in Figure 9a. The graph shows CTF-6 showing maximum stability of 90.5 wt % at the said temperature. Better thermal stability represents better structural integrity and molecular interaction among the constituents of the composite. At 220 °C, the samples that showed good thermal stability after CTF-6 are CTF-8 with 90.2 wt % and CTF-10 with 89.7 wt %. It again proved to have good structural integrity, as mentioned in previous sections. The following composites, CTF-1, CUF-0, and CTF-0.5, were protected by the amino acid bonds of the sericin layer from the extreme burning of the samples. However, due to structural defects, it cannot excel among its other counterparts. CTF-4 showed comparatively better thermal stability (87.2 wt % at 220 °C) because of better interaction among the constituents, as mentioned in previous sections. CTF-2 and CTF-12 showed poor property, probably because of many voids in the CTF-2 structure and thinning of fiber, followed by poor strength for the CTF-12 composite. In the third stage of TGA, the drastic weight reduction occurs above 450 °C, where the remaining N−H, N−O, C−O, and C−O links collapse and the sample completely decompose.[37] Figure 9b shows the enlarged view at 480 °C, where the CTF-6 shows

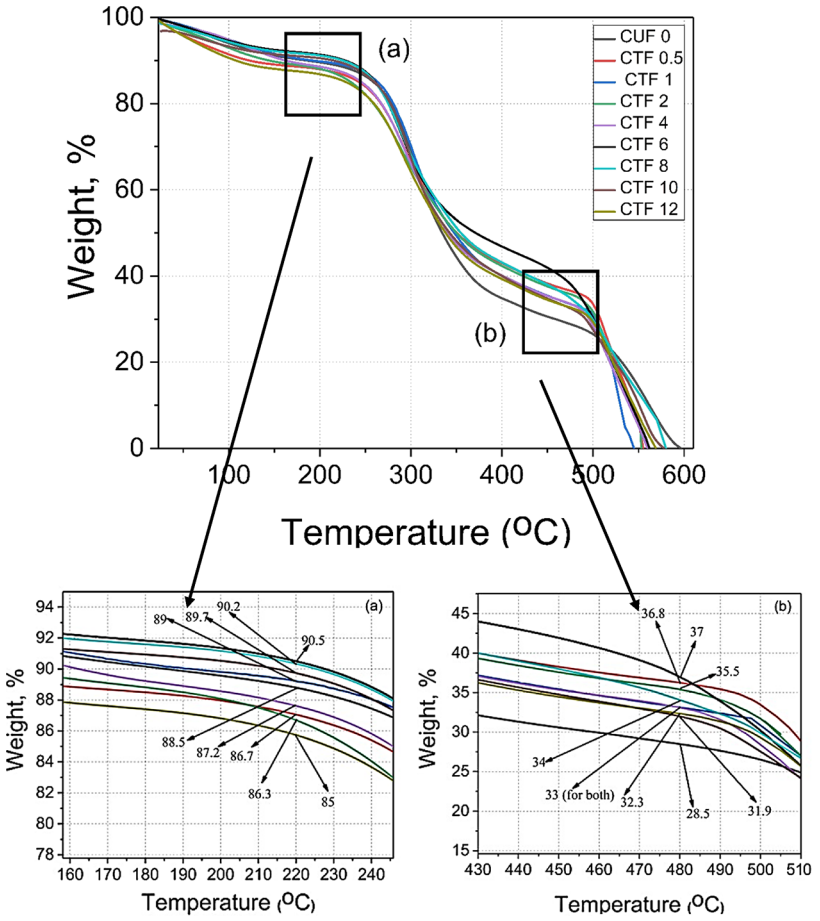

Figure 9. Comparison graph of TGA for the composite manufactured by wheat gluten and untreated and NaOH-treated waste filature silk. (a) Enlarged view at 220 °C and (b) enlarged view at 480 °C.

https://doi.org/10.1021/acsomega.2c05963
ACS Omega 2023, 8, 6268−6278

dominance with 37 wt % over other samples. It is followed by CTF-0.5 at 36.8 wt %, CTF-2 at 35.5 wt %, CTF-8 at 34 wt %, CTF-1 at 33 wt %, CTF-4 at 33 wt %, CTF-12 at 32.3 wt %, CTF-10 at 31.9 wt %, and CTF-0 at 28. 5 wt %. They are all segregated with a very narrow margin showing good thermal stability for all the samples. At the last stage, all the composite samples completely decompose at the temperature range of 550 to 600 °C. Although CTF-6 showed elevated properties for the first three stages, it completely decomposes at 550 °C, which is lesser than CUF-0, CTF-8, CTF-10, and CTF-12. They survived more in the later stage probably because of the presence of the sericin layer, and CTF-8, CTF-10, and CTF-12 survived because of better adhesion among fiber and matrix, which required more energy to burn out completely.

4. APPLICATION

A simple process of surface treatment of the fibers enhanced the physiochemical properties of the composites, which can be further used to develop products of different shapes and sizes. The prepared composite sheets with 6 h of TFs (CTF-6) were molded into different shapes to check their capability to produce sustainable products. The products shown in Figure 10

Figure 10. Plate and pot developed using treated waste filature silk-wheat gluten composite sheets representing the feasibility of preparing various biodegradable products.

represent a biodegradable sampling pot and a disposable plate replicating the similar counterparts available in the market, which is made of plastic. The mechanical testing and TGA studies also showed satisfactory properties, which makes it an excellent candidate to replace plastic disposables like cups and plates. Since the product is entirely biodegradable and non-toxic, it contributes toward clean and green manufacturing. Hot compression molding can easily mold these sheets into different shapes and sizes. They can be commercialized as one-time nursery seedling trays and sampling pots.

5. CONCLUSIONS

In this study, the tensile, impact, thermal and morphological behavior, and molecular spectroscopy were systematically investigated for WG-WFS composites for different durations of fiber treatment in NaOH media. The main findings are as follows,

(i) The XRD study showed increased crystallinity for the degummed fibers as the degumming duration increased. More crystallinity means straighter and lustrous fibers, which helped the composites perform better under tensile and impact loading.

(ii) The FTIR analysis shows enhanced β-sheet formation as the fiber treatment time increases. It supports the enhanced mechanical properties of the TFs for extended hours. On the other hand, shifting peaks to the lower wavenumbers at CTF-6 justifies better interaction among the composite constituents.

(iii) The surface morphology showed enhanced fiber−matrix interaction as the surface of the TFs gradually got degummed. CTF-6 showed the best surface morphology among other composites.

(iv) CUF-0 showed remarkable properties because of the support of the glue-like sericin layer. As the degumming progressed, the composites from CTF-0.5 to CTF-4 showed gradual improvement in their mechanical properties. The overall mechanical properties of CTF 6 excel all other composites in terms of ultimate strength, elongation, and impact energy. However, Young's modulus of sCTF-8 stands highest as more alkali treatment tends to increase the β-sheet formation. The mechanical strength reduces further because of thinning of the fiber due to excessive NaOH exposure.

(v) The TGA showed an almost similar trend for all the composites, but CTF-6 performed marginally better than other composites in terms of thermal stability.

Based on all the thermal and physiochemical observations, it can be concluded that the composite prepared by NaOH-treated WFS for 6 h delivers the best combination of strength, elongation, and thermal properties. This work also provides future possibilities to conduct similar studies using other alkali solutions. The prepared sheets are used to develop 100% degradable nursery seedling pots and trays, which can be directly planted into the soil without discarding the pot.

■ ASSOCIATED CONTENT

Data Availability Statement

Data can be provided if asked.

■ AUTHOR INFORMATION

Corresponding Author

Ravi Kant − *Department of Mechanical Engineering, Indian Institute of Technology Ropar, Ropar 140001 Punjab, India;* orcid.org/0000-0001-5414-4139; Email: ravi.kant@iitrpr.ac.in

Authors

Papiya Bhowmik − *Department of Mechanical Engineering, Indian Institute of Technology Ropar, Ropar 140001 Punjab, India*

Harpreet Singh − *Department of Mechanical Engineering, Indian Institute of Technology Ropar, Ropar 140001 Punjab, India*

https://doi.org/10.1021/acsomega.2c05963
ACS Omega 2023, 8, 6268−6278

Complete contact information is available at:
https://pubs.acs.org/10.1021/acsomega.2c05963

Author Contributions

P.B.: conceptualization, methodology, writing—original draft. R.K.: visualization, supervision, writing—technical review and editing. H.S.: visualization, supervision, writing—technical review and editing.

Funding

No external funding was received for this research.

Notes

The authors declare no competing financial interest.

REFERENCES

(1) Emin, M. A.; Quevedo, M.; Wilhelm, M.; Karbstein, H. P. Analysis of the Reaction Behavior of Highly Concentrated Plant Proteins in Extrusion-like Conditions. *Innovative Food Sci. Emerging Technol.* **2017**, *44*, 15−20.
(2) Guna, V.; Ilangovan, M.; Hu, C.; Venkatesh, K.; Reddy, N. Valorization of Sugarcane Bagasse by Developing Completely Biodegradable Composites for Industrial Applications. *Ind. Crops Prod.* **2019**, *131*, 25−31.
(3) Kunanopparat, T.; Menut, P.; Morel, M. H.; Guilbert, S. Plasticized Wheat Gluten Reinforcement with Natural Fibers: Effect of Thermal Treatment on the Fiber/Matrix Adhesion. *Composites, Part A* **2008**, *39*, 1787−1792.
(4) Hemsri, S.; Grieco, K.; Asandei, A. D.; Parnas, R. S. Wheat Gluten Composites Reinforced with Coconut Fiber. *Composites, Part A* **2012**, *43*, 1160−1168.
(5) Reddy, N.; Yang, Y. Biocomposites Developed Using Water-Plasticized Wheat Gluten as Matrix and Jute Fibers as Reinforcement. *Polym. Int.* **2011**, *60*, 711−716.
(6) Shubhra, Q. T. H.; Alam, A. K. M. M.; Gafur, M. A.; Shamsuddin, S. M.; Khan, M. A.; Saha, M.; Saha, D.; Quaiyyum, M. A.; Khan, J. A.; Ashaduzzaman, M. Characterization of Plant and Animal Based Natural Fibers Reinforced Polypropylene Composites and Their Comparative Study. *Fibers Polym.* **2010**, *11*, 725−731.
(7) Setua, D. K.; Dutta, B. Short Silk Fiber-reinforced Polychloroprene Rubber Composites. *J. Appl. Polym. Sci.* **1984**, *29*, 3097−3114.
(8) Shubhra, Q. T. H.; Alam, A. K. M. M.; Beg, M. D. H. Mechanical and Degradation Characteristics of Natural Silk Fiber Reinforced Gelatin Composites. *Mater. Lett.* **2011**, *65*, 333−336.
(9) Song, R.; Kimura, T.; Ino, H. Papermaking from Waste Silk and Its Application as Reinforcement of Green Composite. *J. Text. Eng.* **2010**, *56*, 71−76.
(10) Sekhar, M. C.; Veerapratap, S.; Song, J. I.; Luo, N.; Zhang, J.; Rajulu, A. V.; Rao, K. C. Tensile Properties of Short Waste Silk Fibers/Wheat Protein Isolate Green Composites. *Mater. Lett.* **2012**, *77*, 86−88.
(11) Bhowmik, P.; Kant, R.; Nair, R.; Singh, H. Influence of Natural Crosslinker and Fibre Weightage on Waste Kibisu Fibre Reinforced Wheatgluten Biocomposite. *J. Polym. Res.* **2021**, *28*, 106.
(12) Priya, S. P.; Ramakrishna, H. V.; Rai, S. K.; Rajulu, A. V. Tensile, Flexural, and Chemical Resistance Properties of Waste Silk Fabric-Reinforced Epoxy Laminates. *J. Reinf. Plast. Compos.* **2005**, *24*, 643−648.
(13) International Sericultural Commission (Inserco). *Statistics | International Sericultural Commission*. 2013.
(14) Hazarika, P.; Hazarika, D.; Kalita, B.; Gogoi, N.; Jose, S.; Basu, G. Development of Apparels from Silk Waste and Pineapple Leaf Fiber. *J. Nat. Fibers* **2018**, *15*, 416−424.
(15) Han, S. O.; Lee, S. M.; Park, W. H.; Cho, D. Mechanical and Thermal Properties of Waste Silk Fiber-Reinforced Poly(Butylene Succinate) Biocomposites. *J. Appl. Polym. Sci.* **2006**, *100*, 4972−4980.
(16) Cao, T. T.; Zhang, Y. Q. Processing and Characterization of Silk Sericin from Bombyx Mori and Its Application in Biomaterials and Biomedicines. *Mater. Sci. Eng. C* **2016**, *61*, 940−952.
(17) Vepari, C.; Kaplan, D. L. Silk as a Biomaterial. *Prog. Polym. Sci.* **2007**, *32*, 991.
(18) Qi, Y.; Wang, H.; Wei, K.; Yang, Y.; Zheng, R. Y.; Kim, I. S.; Zhang, K. Q. A Review of Structure Construction of Silk Fibroin Biomaterials from Single Structures to Multi-Level Structures. *Int. J. Mol. Sci.* **2017**, *18*, 237.
(19) Luo, Y.; Wang, T. Pharmaceutical and Cosmetic Applications of Protein By-Products. In *Protein Byproducts: Transformation from Environmental Burden Into Value-Added Products*; Elsevier Inc., 2016; pp. 147−160
(20) Noreen, A.; Sultana, S.; Sultana, T.; Tabasum, S.; Zia, K. M.; Muzammil, Z.; Jabeen, M.; Lodhi, A. Z.; Sultana, S. Natural Polymers as Constituents of Bionanocomposites. In *Bionanocomposites: Green Synthesis and Applications*; Elsevier, 2020; pp. 55−85.
(21) Hlady, V.; Buijs, J. Protein Adsorption on Solid Surfaces. *Curr. Opin. Biotechnol.* **1996**, *7*, 72−77.
(22) Ranakoti, L.; Gangil, B.; Rajesh, P. K.; Singh, T.; Sharma, S.; Li, C.; Ilyas, R. A.; Mahmoud, O. Effect of Surface Treatment and Fiber Loading on the Physical, Mechanical, Sliding Wear, and Morphological Characteristics of Tasar Silk Fiber Waste-Epoxy Composites for Multifaceted Biomedical and Engineering Applications: Fabrication and Characterizatio. *J. Mater. Res. Technol.* **2022**, *19*, 2863−2876.
(23) Dou, H.; Zuo, B. Effect of Sodium Carbonate Concentrations on the Degumming and Regeneration Process of Silk Fibroin. *J. Text. Inst.* **2015**, *106*, 311−319.
(24) Babu, K. M. The Dyeing of Silk. In *Silk*; Woodhead Publishing, 2019; pp. 109−128
(25) Jiang, P.; Liu, H.; Wang, C.; Wu, L.; Huang, J.; Guo, C. Tensile Behavior and Morphology of Differently Degummed Silkworm (Bombyx Mori) Cocoon Silk Fibres. *Mater. Lett.* **2006**, *60*, 919−925.
(26) Brunsek, R.; Schwarz, I.; Than, M. Mechanical Properties of the Silk Degummed with Citric Acid and Ultrasound. *Funct. Text. Cloth.* **2019**, 131−138.
(27) Heine, E.; Hoecker, H. Bioprocessing for Smart Textiles and Clothing. *Smart Fibres, Fabr. Cloth.* **2001**, 254−277.
(28) Weber, I. E.; Clayton, E. The Hydrogen Peroxide Bleaching of Wool, Cotton, and Silk. *J. Text. Inst. Proc.* **2009**, *24*, 178−193.
(29) Kunz, R. I.; Brancalhão, R. M. C.; Ribeiro, L. D. F. C.; Natali, M. R. M. Silkworm Sericin: Properties and Biomedical Applications. *BioMed Res. Int.* **2016**, 8175701.
(30) Carissimi, G.; Lozano-Pérez, A. A.; Montalbán, M. G.; Aznar-Cervantes, S. D.; Cenis, J. L.; Víllora, G. Revealing the Influence of the Degumming Process in the Properties of Silk Fibroin Nanoparticles. *Polymers* **2019**, *11*, 2045.
(31) Perea, G. B.; Solanas, C.; Marí-Buyé, N.; Madurga, R.; Agulló-Rueda, F.; Muinelo, A.; Riekel, C.; Burghammer, M.; Jorge, I.; Vázquez, J.; Plaza, G. R.; Torres, A. L.; Del Pozo, F.; Guinea, G. V.; Elices, M.; Cenis, J. L.; Pérez-Rigueiro, J. The Apparent Variability of Silkworm (Bombyx Mori) Silk and Its Relationship with Degumming. *Eur. Polym. J.* **2016**, *78*, 129−140.
(32) Gulrajani, M. L. Degumming of Silk. *Rev. Prog. Color. Relat. Top.* **1992**, *22*, 79−89.
(33) Nurazzi, N. M.; Asyraf, M. R. M.; Rayung, M.; Norrrahim, M. N. F.; Shazleen, S. S.; Rani, M. S. A.; Shafi, A. R.; Aisyah, H. A.; Radzi, M. H. M.; Sabaruddin, F. A.; Ilyas, R. A.; Zainudin, E. S.; Abdan, K. Thermogravimetric Analysis Properties of Cellulosic Natural Fiber Polymer Composites: A Review on Influence of Chemical Treatments. *Polymer* **2021**, *13*, 2710.
(34) Vilay, V.; Mariatti, M.; Mat Taib, R.; Todo, M. Effect of Fiber Surface Treatment and Fiber Loading on the Properties of Bagasse Fiber−Reinforced Unsaturated Polyester Composites. *Compos. Sci. Technol.* **2008**, *68*, 631−638.
(35) Ho, M. P.; Wang, H.; Lau, K. T. Effect of Degumming Time on Silkworm Silk Fibre for Biodegradable Polymer Composites. *Appl. Surf. Sci.* **2012**, *258*, 3948−3955.
(36) Lu, S.; Tang, X.; Lu, Q.; Huang, J.; You, X.; Zhang, F. In Vitro and in Vivo Degradation of Silk Fibers Degummed with Various Sodium Carbonate Concentrations. *Mater. Today Commun.* **2021**, *27*, 102369.

(37) Bhowmik, P.; Kant, R.; Nair, R.; Singh, H. The Synergistic Influence of Lemon Extract on the Physio-Chemical Properties of Kibisu Silk Reinforced Wheat Gluten Biocomposite. *Polym. Bull.* **2022**, 1−16.
(38) Haameem, M.; Abdul Majid, M. S.; Afendi, M.; Marzuki, H. F. A.; Fahmi, I.; Gibson, A. G. Mechanical Properties of Napier Grass Fibre/Polyester Composites. *Compos. Struct.* **2016**, *136*, 1−10.
(39) Shahzad, A. Effects of Alkalization on Tensile, Impact, and Fatigue Properties of Hemp Fiber Composites. *Polym. Compos.* **2012**, *33*, 1129−1140.
(40) Oushabi, A.; Sair, S.; Oudrhiri Hassani, F.; Abboud, Y.; Tanane, O.; El Bouari, A. The Effect of Alkali Treatment on Mechanical, Morphological and Thermal Properties of Date Palm Fibers (DPFs): Study of the Interface of DPF−Polyurethane Composite. *South African J. Chem. Eng.* **2017**, *23*, 116−123.
(41) Kumar Dan, A.; Biswal, B.; Das, M.; Parida, S.; Kumar Parhi, P.; Das, D. Aqueous and Chemical Extraction of Saponin of Acacia Concinna (Willd.) Dc.: An Effective Bio-Surfactant Solution to Extract Silk Fibroin from Muga Silk Cocoons. *J. Mol. Liq.* **2022**, *360*, 119547.
(42) Lefèvre, T.; Rousseau, M. E.; Pézolet, M. Protein Secondary Structure and Orientation in Silk as Revealed by Raman Spectromicroscopy. *Biophys. J.* **2007**, *92*, 2885−2895.
(43) Kaewpirom, S.; Boonsang, S. Influence of Alcohol Treatments on Properties of Silk-Fibroin-Based Films for Highly Optically Transparent Coating Applications. *RSC Adv.* **2020**, *10*, 15913−15923.
(44) Chen, X.; Cai, H.; Ling, S.; Shao, Z.; Huang, Y. Conformation Transition of Bombyx Mori Silk Protein Monitored by Time-Dependent Fourier Transform Infrared (FT-IR) Spectroscopy: Effect of Organic Solvent. *Appl. Spectrosc.* **2012**, *66*, 696−699.
(45) Carissimi, G.; Baronio, C. M.; Montalbán, M. G.; Víllora, G.; Barth, A. On the Secondary Structure of Silk Fibroin Nanoparticles Obtained Using Ionic Liquids: An Infrared Spectroscopy Study. *Polymers* **2020**, *12*, 1294.
(46) Arai, T.; Freddi, G.; Innocenti, R.; Tsukada, M. Biodegradation of Bombyx Mori Silk Fibroin Fibers and Films. *J. Appl. Polym. Sci.* **2004**, *91*, 2383−2390.
(47) Nataraj, D.; Sakkara, S.; Meenakshi, H. N.; Reddy, N. Properties and Applications of Citric Acid Crosslinked Banana Fibre-Wheat Gluten Films. *Ind. Crops Prod.* **2018**, *124*, 265−272.
(48) SigmaAldrich. IR Spectrum Table & Chart. *Sigma Aldrich* **2021**, 18.

https://doi.org/10.1021/acsomega.2c05963
ACS Omega 2023, 8, 6268−6278